

Enhancing the oral bioavailability of curcumin using solid lipid nanoparticles

Choongjin Ban^{e,f,1}, Myeongsu Jo^{a,1}, Young Hyun Park^{a,b,c}, Jae Hwan Kim^a, Jae Yong Han^{a,b,c}, Ki Won Lee^{a,d,i,j}, Dae-Hyuk Kweon^{f,g,h}, Young Jin Choi^{a,b,d,*}

^a Department of Agricultural Biotechnology, Seoul National University, 1 Gwanakro, Gwanakgu, Seoul 08826, Republic of Korea

^b Research Institute of Agriculture and Life Sciences, Seoul National University, 1 Gwanakro, Gwanakgu, Seoul 08826, Republic of Korea

^c WCU Biomodulation Major, Seoul National University, 1 Gwanakro, Gwanakgu, Seoul 08826, Republic of Korea

^d Center for Food and Bioconvergence, Seoul National University, 1 Gwanakro, Gwanakgu, Seoul 08826, Republic of Korea

^e Institute of Biomolecule Control, Sungkyunkwan University, Seoburo 2066, Suwon, Gyeonggi 16419, Republic of Korea

^f Biomedical Institute for Convergence, Sungkyunkwan University, Seoburo 2066, Suwon, Gyeonggi 16419, Republic of Korea

^g Department of Integrative Biotechnology, Sungkyunkwan University, Seoburo 2066, Suwon, Gyeonggi 16419, Republic of Korea

^h Interdisciplinary Program in BioCosmetics, Sungkyunkwan University, Seoburo 2066, Suwon, Gyeonggi 16419, Republic of Korea

ⁱ Research Institute of Bio Food Industry, Institute of Green Bio Science and Technology, Seoul National University, Pyeongchang, Republic of Korea

^j Advanced Institutes of Convergence Technology, Seoul National University, Suwon, Republic of Korea

ARTICLE INFO

Keywords:

Curcumin
Oral bioavailability
Solid lipid nanoparticle
Interfacial design
Controllable absorption

ABSTRACT

To control the oral bioavailability of curcumin, we fabricated solid lipid nanoparticles (SLNs) using tristearin and polyethylene glycol (PEG)ylated emulsifiers. Lipolysis of prepared SLNs via simulated gastrointestinal digestion was modulated by altering the types and concentrations of emulsifiers. After digestion, the size/surface charge of micelles formed from SLN digesta were predictable and > 91% of curcumin was bioaccessible in all of the SLNs. The curcumin permeation rate through mucus-covered gut epithelium *in vitro* was dependent on the size/surface charge of the micelles. Curcumin loaded in long-PEGylated SLNs rapidly permeated the epithelium due to the neutral surface charge of the micelles, resulting in a > 12.0-fold increase in bioavailability compared to curcumin solution in a rat model. These results suggest that the bioavailability of curcumin can be controlled by modulating the interfacial properties of SLNs, which will facilitate the development of curcumin formulations for use in functional foods and pharmaceuticals.

1. Introduction

Curcumin, found in turmeric extracted from the rhizome of *Curcuma longa*, can prevent cancers (Strimpakos & Sharma, 2008) and has anti-inflammatory (Julie & Jurenka, 2009), oxygen radical-scavenging (Kunchandy & Rao, 1990), and anti-amyloidogenic effects (Ono, Hasegawa, Naiki, & Yamada, 2004). Additionally, it can be safely consumed by animals and humans based on many studies that have investigated the toxicity (Sharma et al., 2004). Therefore, curcumin could be appropriate as a constituent of functional foods. However, curcumin's low oral bioavailability (OBa), due to its poor water solubility (Anand, Kunnumakkara, Newman, & Aggarwal, 2007), auto-oxidation (Schneider, Gordon, Edwards, & Luis, 2015), instability at neutral/alkaline pH (Wang et al., 1997), active metabolism (Metzler, Pfeiffer, Schulz, & Dempe, 2013), and low permeability across the

apical surface of enterocytes (Wahlang, Pawar, & Bansal, 2011) hampers its use as a bioactive material for functional foods or pharmaceuticals. Therefore, a strategy to overcome these weaknesses of curcumin is needed.

The low OBa of curcumin can be overcome using absorption enhancers and formulation strategies. In preclinical and clinical studies, piperine, as an OBa enhancer, inhibited the activity of metabolic enzymes (Shoba et al., 1998). However, the OBa improvement achieved using enhancers, including piperine, did not reach a satisfactory therapeutic level. Formulation strategies involving nanoparticles (Hartono, Hadisoewignyo, Yang, Meka, & Yu, 2016), curcumin/piperine-co-loaded-nanoparticles (Baspinar, Üstündas, Bayraktar, & Sezgin, 2018), liposomes (Peng et al., 2017), and nanoemulsions (Vecchione et al., 2016) have been proposed to overcome the low OBa of curcumin. These strategies improved the OBa of curcumin, but in all cases the

* Corresponding author at: Department of Agricultural Biotechnology, Seoul National University, 1 Gwanakro, Gwanakgu, Seoul 08826, Republic of Korea.
E-mail address: choijj@snu.ac.kr (Y.J. Choi).

¹ These authors contributed equally to this work.

improvement was demonstrated only *in vitro* or *in vivo*. Additionally, most previous studies did not identify controllable factors influencing the OBA of curcumin. Controlled digestion of emulsions in the gastrointestinal tract (GIT) and solubilization of the encapsulated molecules have been reported (Devraj et al., 2013). Unfortunately, these effects were dependent on the quantities of bile acids (BAs) and calcium ions, which are not controllable factors. Moreover, most studies of controllable digestion overlooked absorption of the bioactives loaded in the carriers through the gut epithelium (Zhang et al., 2016). Thus, further studies of the digestion/absorption of loaded curcumin, and of the factors related to enhancement of its OBA, are needed.

The biocompatible solid lipid nanoparticles (SLNs) can increase the OBA of curcumin (Baek & Cho, 2017). The solid lipid matrix of SLNs immobilizes core materials and protects them against physical/biochemical stressors, such as free radicals, pH, high-ionic-strength solutions, and metabolizing enzymes, during passage through the GIT (Ban, Park, Lim, Choi, & Choi, 2015). Orally ingested bioactive material-loaded SLNs are digested by lipases and form micelles with BAs, phospholipids, and the digestion products, and the bioactives solubilized in the micelles can be absorbed into the lymph through enterocytes (McClements & Xiao, 2012). Additionally, the SLNs enable sustainable release of the core material. Indeed, the OBA of curcumin was enhanced by polyethylene glycol (PEG)ylated SLNs, likely due to sustained release and absorption through the GIT (Ji et al., 2016). However, orally administered SLNs must pass through the digestive tract, which could alter their size, surface charge, and curcumin loading efficiency. Hence, further studies of the digestion/absorption mechanisms are needed to identify controllable factors that allow the limitations of curcumin to be overcome.

We previously suggested that gastrointestinal digestion of SLNs could be controlled using PEGylated emulsifiers, *i.e.*, by altering the length and concentration thereof (Ban, Jo, Lim, & Choi, 2018). Here, we examined if the OBA of curcumin could be increased by PEGylated SLNs and conducted digestion/absorption studies using *in vitro/in vivo* models of the human GIT, to assess the underlying mechanisms. In the *in vitro* digestion study, changes in the size, surface charge, and lipolysis pattern of the SLNs were recorded after treatment with digestion fluid, and the amount of solubilized curcumin in the mixed micellar fraction was determined. In the absorption study, gut permeation of curcumin loaded in SLNs was assessed using mucus-covered Caco-2 cell monolayers, and a pharmacokinetics study was performed in a rat model.

2. Materials and methods

2.1. Chemicals

Tristearin (TS), polyoxyethylene (10) stearyl ether (PEG10SE; Brij® S10), polyoxyethylene (100) stearyl ether (PEG100SE; Brij® S100), bovine serum albumin (BSA), polyacrylic acid, cholesterol, polysorbate 80, mucin, and phosphatidylcholine were purchased from Sigma Aldrich Co. (St. Louis, MO, USA). Liquid canola oil (LCO) was obtained from CJ Cheiljedang Co. (Seoul, South Korea). Curcumin and linoleic acid were supplied by Acros Organics (Pittsburg, PA, USA) and Tokyo Chemical Industry (Tokyo, Japan), respectively. Eagle's minimum essential medium (EMEM) and fetal bovine serum (FBS) were purchased from the American Type Culture Collection (ATCC, Manassas, VA, USA) and GE Healthcare (Chicago, IL, USA), respectively. Nonessential amino acids (NEAA), antibiotic-antimycotic, trypsin-ethylenediaminetetraacetic acid (EDTA), and Hank's balanced salt solution (HBSS) were obtained from Thermo Fisher Scientific (Waltham, MA, USA). All other chemicals were of analytical-reagent grade.

2.2. Fabrication of solid lipid nanoparticles and emulsion

The curcumin-loaded SLNs/emulsion were prepared using an oil-in-water emulsion technique, as reported previously (Ban, Lim, Chang, &

Choi, 2014) but with slight modifications. First, the lipid (5 wt%) and aqueous (95 wt%) phases were heated to 85 °C and mixed using a high-speed blender (Ultra-Turrax T25D; Ika Werke GmbH & Co., Staufen, Germany) at 8,000 rpm for 1 min followed by at 11,000 rpm for 1 min. The lipid phase of the curcumin-loaded SLNs was prepared by blending TS (95 wt% of the lipid phase) and curcumin (5 wt% of the lipid phase) in ethanol (25 mg mL⁻¹) and evaporating the ethanol with stirring for 30 min (85 °C). The aqueous phase was fabricated by dissolving PEG10SE or PEG100SE (5.3–46.9 mM) in double-deionized water (DDW) with stirring for 1 h. After preparing the coarse emulsion, the droplet size was reduced by sonication (VCX 750; Sonics & Materials Inc., Newtown, CT, USA) for 4 min at 60% amplitude, with a temperature of 85 °C and a duty cycle of 1 s. Next, sonication was performed for 6 min was applied to the emulsions during cooling to 45 °C, and the samples were immediately stored at 4 °C. The curcumin-loaded emulsion was prepared in the same manner as the curcumin-loaded SLN stabilized by 46.9 mM PEG10SE, except that LCO was used in place of TS.

2.3. Characterization of solid lipid nanoparticles and emulsion

Solid lipid nanoparticles diluted 10-fold with DDW were passed through a 1 µm pore-size filter (GF/B; Whatman Ltd., Loughborough, UK). The aggregated SLNs (> 1 µm) remaining on the filter were weighed after drying in an oven at 60 °C. The difference in filter weight before and after this procedure, *i.e.*, the weight of the aggregated SLNs, was recorded and the yield was calculated as the percentage of the filter weight difference per the SLN weight. To measure the mean particle size (PS, z-average) and ζ-potential (ZP), using a Zetasizer with a 173° angle helium–neon laser (λ = 633 nm; Nano ZS; Malvern Instruments Ltd., Worcestershire, UK), the SLNs and emulsion were passed through filters to eliminate aggregates. The ZP measurement was based on the Smoluchowski equation at 25 °C with an electric field strength of 20 V cm⁻¹.

Emulsifier surface load (Γ_s) was calculated as Γ_s = C_aD/6Φ, where C_a is the concentration of the emulsifier adsorbed to the surface of the SLNs/emulsion, D is the PS, and Φ is the lipid phase volume fraction (*i.e.*, 0.05). The method for determining C_a was introduced previously by our group (Ban et al., 2018). Briefly, emulsifier not coating the lipid particles/droplets was collected using a Sephadex G-25 column (GE Healthcare, Chalfont St. Giles, UK) and quantified using ammonium cobalt thiocyanate (ACTC) solution and a spectrophotometer (Pharmaspec UV-1700; Shimadzu Corp., Kyoto, Japan). The C_a for the SLNs/emulsion was calculated by subtracting the non-coating emulsifier concentration from the total concentration of emulsifiers.

To solubilize untrapped curcumin and precipitate the curcumin-loaded particles/droplets, 0.2 mL of the SLN/emulsion dispersion was added to a 1.8 mL mixture of methanol and acetonitrile (1:1), vortexed for 10 s, and centrifuged (15,000 rcf, 10 min; 5427R; Eppendorf AG, Hamburg, Germany). The supernatant was filtered through a 0.22-µm polyvinylidene difluoride (PVDF) membrane (Millex-GV 33MM syringe filter; Merck Millipore, Bedford, MA, USA) and curcumin was quantified by high-performance liquid chromatography (HPLC; 3.125–100 µg mL⁻¹, R² = 1.0000; λ = 426.9 nm). The entrapment efficiency (EE) of the curcumin-loaded SLNs/emulsion was determined using the equation:

$$EE(\%) = \frac{W_t - W_s}{W_t} \times 100$$

where W_t is the total weight of curcumin and W_s is the weight of curcumin in the supernatant (*i.e.*, the weight of untrapped curcumin).

2.4. High-performance liquid chromatography

A HPLC system equipped with a Waters 2695 Separations module (Waters, Milford, MA, USA) and analytical C18 column (Venusil XBP

C18, 5 μm , 100 \AA , 4.6 \times 250 mm; Bonna-Agela Technology, Newark, DE, USA) was utilized for curcumin quantification. Detection was conducted at 25 $^{\circ}\text{C}$ using a Waters 996 Photodiode Array Detector. Curcumin in the samples (20 μL) was isocratically eluted at a flow rate of 0.8 mL min^{-1} using a mixture (35:55:10) of methanol, acetonitrile, and 5 vol% acetic acid as the mobile phase. This HPLC system was used for quantification of curcumin, the soluble fraction in the mixed micelles, permeation via the simulated gut membrane, and pharmacokinetic analysis.

2.5. Measurement of the size and ζ -Potential of the solid lipid nanoparticles and emulsion after simulated gastrointestinal digestion

Prior to determination of the colloidal stability of SLNs/emulsion under high ionic strength/acidic conditions, the SLNs/emulsion were diluted 10-fold and aggregates were eliminated by filtration (1 μm). To set high ionic strength conditions, 5 mL of the diluted/filtered SLNs/emulsion was blended with 3.8 mL of the mixture of all media and juices, except HCl solution, proteins, bile, and enzymes (Table S1). The mixture was adjusted to pH 7 using 1 M NaOH or 1 M HCl solution and a pH meter (Professional Meter PP-15; Sartorius AG, Göttingen, Germany). For acidic conditions, the diluted/filtered dispersions were adjusted to pH 3 using 50 mM HCl and incubated in a shaking water bath (BS-31; JEIO Tech., Seoul, South Korea) (2 h, 37 $^{\circ}\text{C}$, 100 rpm). Next, 2 mL of the samples were centrifuged (10 min, 25,000 rcf; Eppendorf 5427R) to eliminate creamed SLN aggregates. The PS and ZP of SLNs/emulsion in the supernatant were measured using the Zetasizer. The relative centrifugal force (25,000 rcf) was determined in preliminary experiments and did not induce creaming or sedimentation of freshly prepared SLNs/emulsion.

To determine the effects of pancreatic-lipase and BA on changes in the PS and ZP of SLNs/emulsion, 5 mL of diluted (10-fold) and filtered (1 μm) SLNs/emulsion was treated with pancreatic lipase (3.965 mg mL^{-1}), bile extract (41.32 mg mL^{-1}), and a mixture of lipase and bile. After incubation for 2 h at 37 $^{\circ}\text{C}$ with shaking at 100 rpm, 2 mL samples were centrifuged for 10 min at 25,000 rcf to eliminate creamed SLN aggregates. The PS and ZP of SLNs/emulsion in the supernatant were measured using the Zetasizer.

The *in vitro* digestion test model was developed by our group (Ban et al., 2015), and the digestion medium/juices used are described in Table S1:

- (I) Preingestion: SLNs/emulsion were passed through a filter with a 1 μm pore size.
- (II) Mouth (pH 7; 5 min): 5 mL amounts of the dispersions were mixed with 6 mL of simulated salivary medium.
- (III) Stomach (pH 3; 2 h): 12 mL of simulated gastric juice was added.
- (IV) Small intestine (pH 6.5–7; 2 h): simulated duodenal juice (12 mL), bile juice (6 mL), and NaHCO_3 solution (2 mL) were added.

The samples were incubated with shaking at 37 $^{\circ}\text{C}$ and 100 rpm during *in vitro* digestion to mimic GIT motility. After each digestion step (I–IV), the digesta (2 mL) was centrifuged (10 min, 25,000 rcf) to ensure reliability by negating any effect of creamed SLN aggregates. The PS and ZP of particles in the supernatant were measured using the Zetasizer.

2.6. Determination of the soluble percentage of curcumin after simulated gastrointestinal digestion

After *in vitro* digestion, the soluble percentage of curcumin in the digesta (bioaccessibility, %) was determined (Fig. S1). Briefly, the digesta (43 mL) was centrifuged for 30 min at 1500 rcf and 4 $^{\circ}\text{C}$ to separate out insoluble substances (Supra 22 K; Hanil Science Industrial Co., Seoul, South Korea), and the first supernatant was centrifuged for 20 min at 16,000 rcf and 4 $^{\circ}\text{C}$. The first and second pellets were carefully washed

twice with DDW. A mixture of methanol, acetonitrile, and DDW (43 mL; 45:45:10) was then added, and the pellets were sonicated to dissolve insoluble curcumin and centrifuged for 20 min at 16,000 rcf and 4 $^{\circ}\text{C}$ to precipitate insoluble impurities. For the first and second pellets, the curcumin concentrations in the impurity-eliminated supernatant were determined by HPLC quantification (3.125–100 $\mu\text{g mL}^{-1}$, $R^2 = 1.0000$; $\lambda = 426.9 \text{ nm}$) after filtration through a 0.22- μm PVDF membrane (Millex-GV; Millipore), and were referred to as C_{p1} and C_{p2} , respectively.

The second supernatant (0.2 mL) was diluted 10-fold with mixed organic solvent (1.8 mL of methanol and acetonitrile; 1:1) and sonicated to dissolve the curcumin solubilized in mixed micelles. After centrifugation for 20 min at 16,000 rcf and 4 $^{\circ}\text{C}$ to eliminate impurities, the supernatant was passed through the PVDF membrane. The curcumin concentration (C_{s2}) was then determined by HPLC quantification. The bioaccessibility(%) of curcumin in the digesta was calculated using the following equation:

$$\text{Bioaccessibility(\%)} = 100 \times \frac{10C_{s2}}{C_{p1} + C_{p2} + 10C_{s2}}$$

where ($C_{p1} + C_{p2}$) and ($10C_{s2}$) are the concentrations of insoluble and soluble curcumin, respectively. In addition to the curcumin-loaded SLNs and emulsion, equivalent concentrations (500 $\mu\text{g mL}^{-1}$) of curcumin, diluted with 5 vol% ethanol, were investigated.

2.7. Cumulative release of curcumin from solid lipid nanoparticles

The cumulative release of curcumin from the matrix of SLNs and emulsion was studied using dialysis bags with a 12 kDa molecular-weight cut-off. After being immersed overnight in DDW, the bags were filled with 5 mL of curcumin-loaded SLNs, tightly sealed, suspended in 45 mL of the mixture (1:1) of enzyme-free *in vitro* digestion medium mixture and methanol, and incubated at 100 rpm in a 37 $^{\circ}\text{C}$ water bath. At predetermined time points, a 1 mL aliquot was withdrawn from the medium mixture, and 1 mL of fresh medium was added immediately. Next, the absorbance of the aliquot was recorded using a spectrophotometer. The concentrations of curcumin in the aliquots were calculated (0.25–4.0 $\mu\text{g mL}^{-1}$, $\lambda = 429 \text{ nm}$, $R^2 = 0.9999$).

2.8. Monitoring the lipolysis pattern of the solid lipid nanoparticles and emulsion during simulated Small-intestinal digestion

The lipolysis patterns of the SLNs and emulsion were monitored for 2 h at 37 $^{\circ}\text{C}$ using a titration method described previously (Ban et al., 2015). The simulated small-intestinal fluid was prepared by dissolving sodium chloride, calcium chloride, bile extract, and pancreatic-lipase in 10 mM sodium phosphate buffer (pH 7) at 43.83, 11.098, 100, and 12 mg mL^{-1} , respectively, and adjusting to pH 7 using 1 M NaOH. Prior to titration, the SLNs and emulsion were diluted 10-fold with 10 mM sodium phosphate buffer (pH 7) and adjusted to pH 7 using 0.1 M NaOH. Lipolysis was monitored by measuring free fatty acid (FFA) release from the samples after addition of fluid. The amount of FFAs produced was quantified by adding 0.05 M NaOH to the reaction vessel using an automatic titration unit (842 Titrand; Metrohm AG, Herisau, Switzerland) to maintain the pH at 7, and was converted into %FFA using the following equation:

$$\% \text{FFA} = 100 \times \frac{V_{\text{NaOH}} \times m_{\text{NaOH}} \times M_{\text{Lipid}}}{w_{\text{Lipid}} \times 2}$$

where V_{NaOH} is the volume (L) of the NaOH solution consumed to neutralize the FFAs, m_{NaOH} is the molarity (0.05 mol L^{-1}) of the NaOH solution, M_{Lipid} is the molecular weight (TS, 891.45 g mol^{-1} ; LCO, 876.6 g mol^{-1}) of lipids, and w_{Lipid} is the total weight (0.1 g) of lipids initially present in the reaction vessel. Blank experiments involved the simulated fluid containing heat-inactivated lipase (95 $^{\circ}\text{C}$, 30 min), to

exclude a change in pH due to other factors. The area under the %FFA curve ($AUC_{120 \text{ min}}$) values in the SLN or emulsion system were calculated using the following equation:

$$\sum_{n=1}^{24} \frac{1}{2} \times (\%FFA_{n-1} + \%FFA_n) \times \Delta t$$

where n is the unit for the module divided into 5-min blocks and Δt is the time between adjacent modules (5 min).

2.9. Permeation of curcumin across a simulated gut membrane

Permeation experiments were conducted to assess the epithelial absorption of curcumin in the digesta after 2-h lipolysis assay. The reaction was terminated by adding 60.25 μL of 4-bromophenylboronic acid solution (0.5 μM). The dispersions after 2-h lipolysis assay without lipase or lipase/bile extract were used for comparison. The simulated mucus contained 0.9% (w/v) polyacrylic acid, 5% (w/v) mucin, 3.1% (w/v) BSA, 0.11% (w/v) linoleic acid, 0.36% (w/v) cholesterol, 0.18% (w/v) phosphatidylcholine, and 0.16% (w/v) polysorbate 80 (Boegh, Baldursdóttir, Müllertz, & Nielsen, 2014). Under stirring, linoleic acid, cholesterol, phosphatidylcholine, and polysorbate 80 were mixed in 10 mM 4-(2-hydroxyethyl)-1-piperazineethanesulfonic acid (HEPES) buffer (pH 6.5), blended with polyacrylic acid and mucin, and then mixed with BSA. The pH was adjusted to 6.5 with 1 M HCl or 1 M NaOH solution as necessary. The mucus was stored overnight at 4 °C. Caco-2 cells (HTB-37) obtained from the ATCC were cultured in 88% EMEM, 10% FBS, 1% NEAA, and 1% antibiotic solution at 37 °C and 5% CO_2 . Cells at passages 10–12 were used in this study and were harvested using trypsin-EDTA.

The harvested Caco-2 cells were transferred to polycarbonate membrane Transwell inserts (pore size, 0.4 μm ; Corning Costar Inc., Corning, NY, USA) for 12-well plates at a density of 3×10^5 per insert. The culture medium was replaced every other day. Twenty-one days later, Caco-2 cells were washed with HBSS (pH 7.4) to remove cell debris and incubated (15 min, 37 °C) with 500 and 1500 μL of HBSS in the apical and basolateral compartments, respectively. After discarding the HBSS, 250 μL of mucus was added to Caco-2 cell monolayers in the apical compartment, and the sample was diluted fivefold by adding buffer solution into the apical (pH 6.5; 250 μL) or basolateral compartment (pH 7.4; 1500 μL). Buffer solution (pH 7.4) was prepared by mixing HEPES (20 mM), NaHCO_3 (0.35 mg mL^{-1}), and BSA (4% w/v) in HBSS and filtered through a 0.22- μm PVDF membrane, which was acidified with methanesulfonic acid (10 mM) to a pH of 6.5 as necessary. Next, 1500 μL of buffer solution (pH 7.4) was added to the basolateral compartment for the apical-to-basolateral (A-B) permeation assay and 250 μL of buffer solution (pH 6.5) was added to the apical compartment for the basolateral-to-apical (B-A) assay. The plate was covered with a lid and incubated in a horizontal shaker for 15, 30, 45 and 60 min at 37 °C with shaking at 100 rpm. Next, the buffer solution in the compartment opposite the sample was collected and replaced immediately with fresh buffer solution (A-B, 300 μL basolateral; B-A, 100 μL apical). In assays without mucus, 400 and 1200 μL of the donor or receiver solution was added to the apical and basolateral compartments, respectively, and 100 and 300 μL of the apical and basolateral compartment solution was collected and replaced, respectively, at the predetermined time.

The collected solutions were diluted twofold with a mixture (45:45:10) of methanol, acetonitrile, and DDW, centrifuged (10 min, 25,000 rcf, 25 °C; Eppendorf 5427R), and filtered through a 0.22- μm PVDF membrane. The amount of curcumin in the solutions was determined by HPLC. The apparent permeability coefficient (P_{app} , cm s^{-1}) was calculated by the equation (Hubatsch, Ragnarsson, & Artursson, 2007):

$$P_{\text{app}} = \frac{dQ}{dt} \times \frac{1}{AC_0}$$

where dQ/dt is the curcumin permeation rate ($\mu\text{g s}^{-1}$), A is the surface area of the insert membrane (1.1 cm^2), and C_0 is the initial concentration of curcumin in the donor solution ($\mu\text{g mL}^{-1}$).

2.10. Pharmacokinetics study

Male Sprague–Dawley rats (250–300 g) were euthanized for *in vivo* pharmacokinetics studies. The pharmacokinetic procedure was approved by the Institutional Animal Care and Use Committee of Seoul National University, Seoul, South Korea (registration number, SNU-160316-1). The rats were divided into six groups ($n = 9$). Group 1 was administered 50 mg kg^{-1} body weight (BW) curcumin dissolved in 5 vol% ethanol, and group 2 received 25 mg kg^{-1} BW curcumin loaded into the emulsion. Groups 3 and 4 were administered 25 mg kg^{-1} BW curcumin loaded in SLNs stabilized by 17.1 and 46.9 mM PEG10SE, respectively, and groups 5 and 6 were administered 25 mg kg^{-1} BW of curcumin encapsulated in SLNs stabilized by 17.1 and 46.9 mM PEG100SE, respectively, by oral gavage. After administration, a 0.4 mL blood sample was collected from the caudal vein into tubes containing K_2EDTA . Next, 0.5 mL of dextrose normal saline was administered to prevent changes in the central compartment volume and electrolytes. Plasma was obtained by centrifugation of blood for 10 min at 4000 rcf and 4 °C. Next, 25 μL of 2.8% acetic acid was added to 200 μL of plasma for curcumin stabilization; 50 μL of β -estradiol 17-acetate (100 $\mu\text{g mL}^{-1}$ ethanol) as the internal standard was then added, and the mixture was vortexed for 20 s. To reduce the noise caused by serum impurities, an extraction was conducted by adding 1 mL of ethyl acetate and vortexing for 10 min. The extract was centrifuged for 10 min at 10,000 rcf and 4 °C. The organic layer containing curcumin and β -estradiol 17-acetate was collected and evaporated for 40 min in a centrifugal evaporator (CVE-2200; Tokyo Rikakikai Co., Ltd., Tokyo, Japan), reconstituted in 200 μL of a mixture (45:45:10) of methanol, acetonitrile, and DDW, and analyzed by HPLC (6.25–200 ng mL^{-1} , $R^2 = 0.9985$; $\lambda = 425 \text{ nm}$).

Pharmacokinetic parameters were calculated based on the plasma pharmacokinetics of curcumin. The peak concentration (C_{max}) and time to the peak concentration (t_{max}) were obtained from the individual profiles. The area under the curve from 0 to 9 h ($AUC_{0-9\text{h}}$) was determined using a trapezoidal rule. $AUC_{0-\infty}$, the area under the profile from time 0 to infinity, was determined as:

$$AUC_{0-\infty} = AUC_{0-9\text{h}} + C_t/K_e$$

where C_t is the curcumin concentration at the last time point and K_e is the apparent elimination rate constant obtained from the terminal slope of the individual profile. Based on the $AUC_{0-\infty}$, relative bioavailability was defined as the $AUC_{0-\infty}$ of the individual groups relative to the $AUC_{0-\infty}$ of group 1.

2.11. Statistical analysis

The $AUC_{120 \text{ min}}$ and pharmacokinetics data were analyzed by Tukey least significant difference test using IBM SPSS Statistics software (version 21.0; IBM Corp., Armonk, NY, USA). Data are means of at least three independent experiments. A value of $p < 0.05$ was considered indicative of statistical significance.

3. Results

3.1. Characteristics of the solid lipid nanoparticles and emulsion

The appearance of SLN dispersions was evaluated (Fig. S2). Most SLNs produced were opaque regardless of the emulsifier type (PEG10SE or PEG100SE), due to light scattering by large particles. However, SLNs stabilized by 46.9 mM PEG10SE and PEG100SE were translucent despite having the same lipid content (5 wt%) as the opaque dispersions, indicating that the SLNs were small. Meanwhile, the SLNs were well-dispersed and spherical or polyhedral, irrespective of the type or

Table 1

Yield, particle size (PS), ζ -potential (ZP), surface load (Γ_s), and entrapment efficiency (EE) of curcumin-loaded emulsion and tristearin nanoparticles stabilized by PEG10SE^a and PEG100SE^b.

Samples	Surfactant concentration (mM)	Yield (%)	PS (nm)	ZP (mV)	Γ_s (nm ⁻²) ^c	EE (%)
Emulsion ^d	46.9	–	111.80 ± 3.29	–6.70 ± 1.00	3.10	91.04 ± 0.26
PEG10SE	5.3	60.99	346.00 ± 1.59	–27.00 ± 0.26	1.03	93.19 ± 0.03
	17.1	83.34	271.97 ± 4.36	–16.53 ± 0.29	2.26	93.26 ± 0.02
	25.6	91.20	243.67 ± 1.97	–13.83 ± 0.72	3.23	93.29 ± 0.01
	34.1	94.02	215.40 ± 1.25	–12.57 ± 0.29	3.30	94.51 ± 0.01
	46.9	95.20	121.03 ± 1.23	–8.26 ± 0.25	3.37	94.04 ± 0.02
PEG100SE	5.3	93.83	242.17 ± 2.57	–8.80 ± 0.46	0.74	91.15 ± 0.09
	17.1	94.30	208.73 ± 9.03	–7.83 ± 0.23	1.82	91.74 ± 0.77
	25.6	94.81	197.33 ± 3.56	–3.80 ± 0.23	2.24	94.74 ± 0.21
	34.1	95.79	189.90 ± 5.78	–1.59 ± 0.28	3.25	93.79 ± 0.67
	46.9	95.79	147.80 ± 1.90	–1.18 ± 0.39	3.27	92.55 ± 0.20

^a polyethylene glycol (10) stearyl ether.

^b polyethylene glycol (100) stearyl ether.

^c The number of emulsifiers adsorbing on the surface unit (1 nm²) of the tristearin matrix.

^d Curcumin-loaded emulsion prepared with liquid canola oil.

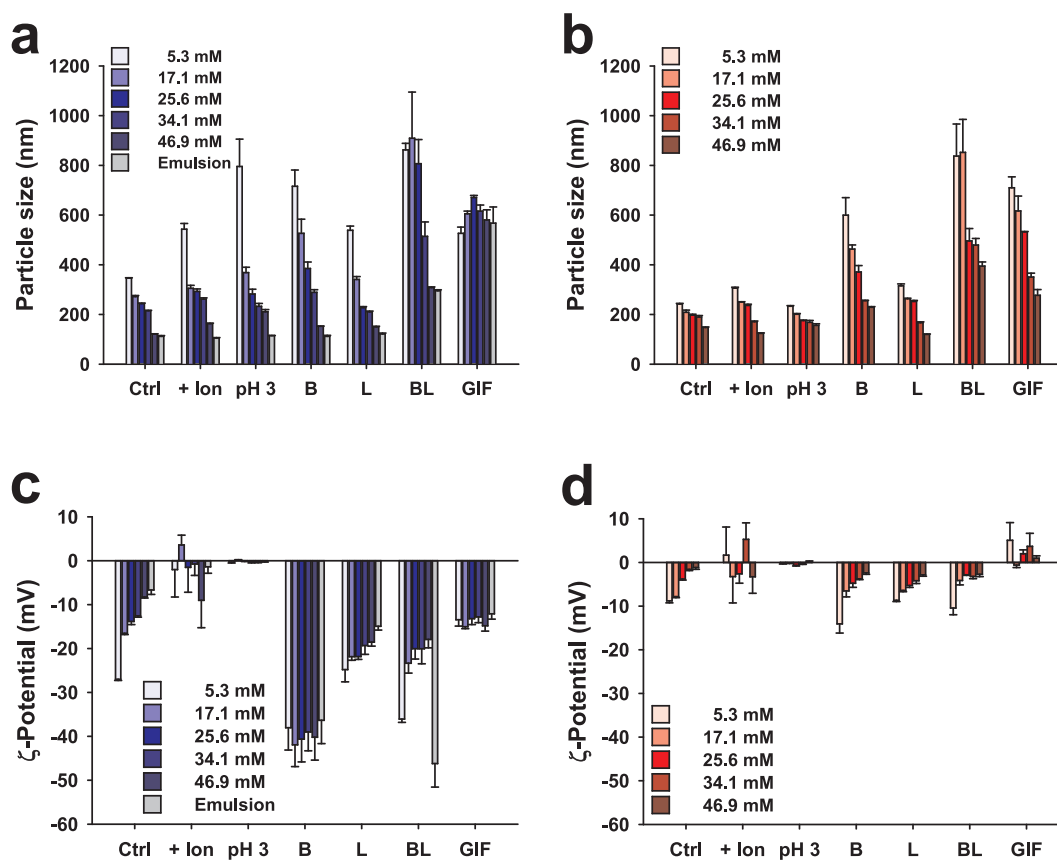


Fig. 1. Particle size (PS, z-average) and ζ -potential (ZP) of curcumin-loaded tristearin (TS) nanoparticles and emulsion stabilized by (a and c) PEG10SE and (b and d) PEG100SE after treatment (2 h) with a high ionic strength solution (+ion), acid (pH 3), bile extract (B), pancreatic lipase (L), a mixture of bile extract and pancreatic lipase (BL), or gastrointestinal fluid (GIF; saliva fluid → gastric fluid → small-intestinal fluid).

concentration of emulsifiers used (Fig. S3).

The physicochemical properties (yield, PS, ZP, and Γ_s) of the SLNs and emulsion were determined (Table 1). Irrespective of the emulsifier type, the yield and Γ_s of the SLNs increased as the emulsifier concentration increased from 5.3 to 46.9 mM, indicating enhanced colloidal stability (PEG10SE, 60.99–95.20% and 1.03–3.37 nm⁻²; PEG100SE, 93.83–95.79% and 0.74–3.27 nm⁻²). The PS of the SLNs decreased as the concentration increased (PEG10SE, 346.00–121.03 nm; PEG100SE, 242–147.80 nm), and neutralization of ZP increased with more emulsifiers (PEG10SE, –27.00 to –8.26 mV; PEG100SE, –8.80 to –1.18 mV), due to reduced surface tension and

greater coating by the emulsifiers, respectively. At low emulsifier concentrations (5.3–25.6 mM), the yield of PEG10SE-stabilized SLN was lower than that of PEG100SE-stabilized SLN, due to more effective steric hindrance by PEG100SE at the TS-water interface. The PS of PEG10SE-stabilized SLNs was more sensitive to changes in the emulsifier concentration than that of PEG100SE-stabilized SLNs, possibly due to the different diffusion coefficients of PEG10SE and PEG100SE (Tadros, Izquierdo, Esquena, & Solans, 2004). Additionally, at the same emulsifier concentration, the ZP of PEG10SE-stabilized SLNs was more negative than that of PEG100SE-stabilized SLNs, and the Γ_s of PEG10SE-stabilized SLNs was larger than that of PEG100SE-stabilized SLNs. This

indicates more effective coverage of PEG100SE than of PEG10SE, neutralizing the negative charge resulting from impurities. According to the EE results (> 91%), there was no relationship between curcumin loading in SLNs and emulsifier concentration or type.

Thermographs were obtained to determine the thermal properties of SLNs and their constituents (Fig. S4). The emulsifiers used did not melt or crystallize under aqueous conditions (Fig. S4h-k). In this respect, the peaks in the thermographs of the SLN dispersions (Fig. S4i-o) were attributed to the melting and crystallization of TS. In the thermograph of supercooled bulk TS (Fig. S4a2), peaks at 50 and 59 °C represented the α - and β '-formed crystals of TS, respectively. Thus, TS matrices within SLNs stabilized by 5.3 and 46.9 mM PEG10SE and PEG100SE were present as β '- and α -formed crystals, respectively. The yield, PS, ZP, Γ_s , and EE of the curcumin-loaded LCO emulsion were similar to those of 46.9 mM PEG10SE-stabilized SLNs, because the same emulsifier concentration was used.

3.2. Digestion of solid lipid nanoparticles and emulsion in the gastrointestinal tract

Changes in PS and ZP were monitored to assess the colloidal stability of the SLNs and emulsion under various digestion conditions in the GIT. Under the high-ionic-strength and acidic conditions, only minor size increases were identified in most SLNs/emulsion, with the exception of the 5.3 mM PEG10SE-stabilized SLN (Fig. 1a and b; Fig. S5), despite the almost neutralized ZP (Fig. 1c and d). The creamed aggregates of 5.3 mM PEG10SE-stabilized SLNs could be identified with the naked eye. After bile extract treatment, the ZP of all PEG10SE-stabilized SLNs/emulsion decreased to ~ -40 mV due to the adsorption of BA (-52 mV) at the interface, and size increases were observed in < 34.1 mM PEG10SE-stabilized SLNs. However, in PEG100SE-stabilized SLNs, only the ZP of 5.3 mM PEG100SE-stabilized SLNs decreased, to -14 mV. The size of all SLNs increased slightly, indicating little adsorption of BA at the interface. After pancreatic-lipase treatment, the ZP of the PEG10SE-stabilized SLNs/emulsion slightly decreased, and that of the PEG100SE-stabilized SLNs remained stable, resulting in a slightly increased size of the < 17.1 mM PEG10SE-stabilized SLNs. After treatment with the mixture of bile extract and pancreatic lipase, the size of all SLNs/emulsion increased by more than twofold; only the ZP of PEG10SE-stabilized SLNs/emulsion was decreased due to adsorption of BAs at the interface. Additionally, after each *in vitro* digestion step (mouth and stomach), the PS of all samples was almost unchanged, with the exception of the increased PS of 5.3 mM PEG10SE-stabilized SLN, despite the ZP neutralization (Fig. S6). After *in vitro* digestion in the gastrointestinal fluids (GIFs), the ZP of PEG10SE-stabilized SLNs/emulsion and PEG100SE-stabilized SLNs were ~ -14 and ~ 0 mV, respectively, due to BA adsorption and the high ionic strength, and size increases were observed in all SLNs/emulsion.

The cumulative release pattern of encapsulated curcumin can provide information on curcumin leakage not induced by particle hydrolysis during GIT digestion. This can be used to determine the location of curcumin in the lipid matrix and the encapsulation efficacy of the matrix (Higuchi, 1963). < 40% of the overall amount of amount was released from all of the SLN matrices for 12 h, despite the favorable release conditions conferred by the 50 vol% ethanol solution (Fig. 2a and b). After fitting to the Higuchi equation ($Q = K_H t^{1/2}$; Q, cumulative percentage of curcumin release; K_H , Higuchi constant; t , time; $R^2 > 0.92$, $p < 0.0001$), the K_H values of the PEG10SE-stabilized SLNs were larger than those of PEG100SE-stabilized SLNs under the same emulsifier concentration, indicating more rapid release of curcumin from PEG10SE-stabilized SLNs. This also implies that the larger PEG molecules of PEG100SE cover more of the particle. Moreover, irrespective of the emulsifier type, the K_H decreased with increasing emulsifier concentration due to the coverage of the emulsifiers at the interface.

We evaluated the lipolysis profiles of the SLNs and emulsion in the

in vitro small-intestinal fluid (Fig. 2c and d), and the extent of lipolysis was given by the $AUC_{120 \text{ min}}$ value (Fig. 2e). At the start of digestion, the emulsion had the highest lipolysis rate and $AUC_{120 \text{ min}}$ value. For the PEG10SE-stabilized SLNs, the initial lipolysis rate and the $AUC_{120 \text{ min}}$ increased with increasing emulsifier concentration. Use of high concentration of PEG10SE decreased the size and increased the interfacial area, resulting in the increases in initial lipolysis rate and $AUC_{120 \text{ min}}$. Conversely, for the PEG100SE-stabilized SLNs, the initial lipolysis rate was similar irrespective of concentration, but the $AUC_{120 \text{ min}}$ decreased as the emulsifier concentration increased, possibly due to the increased Γ_s , rather than the decreased size, of the SLNs (Ban et al., 2018). The mixed micelle-like nanostructures formed after titration were of submicron size and spherical in shape (Fig. S7).

After digestion of the SLNs and emulsion in the *in vitro* GIT, the soluble curcumin in the digested micellar fraction was evaluated in terms of the bioaccessibility (%) (Fig. 2f). The bioaccessibility of powdered curcumin was 14%, meaning that 86% was insoluble, but this increased to 82% for curcumin dissolved in 5 vol% ethanol. The bioaccessibility of the SLNs/emulsion was in the range of 92–95%, indicating that most of the curcumin in the SLNs and emulsion was soluble in the micellar fraction after digestion in the GIT.

3.3. Absorption of curcumin via the Small-intestinal epithelium

Curcumin uptake in the small intestine was evaluated using Caco-2 cell monolayers covered with an artificial mucus layer. The presence of a Caco-2 cell monolayer was verified by fluorescence microscopy (Fig. S8a), and the mucus layer was assessed in terms of its viscosity and storage and loss moduli (Fig. S8b and c). After the curcumin permeation study using the mucus-covered monolayer, the *trans*-epithelial electrical resistance (TEER) was maintained at 263–269 m Ω (Fig. S8d) (Boegh et al., 2014). Based on measurement of the amount of curcumin (Figs. S9 and S10), the P_{app} was determined (Figs. 3 and S10). The upper (apical) and lower (basolateral) compartments of the membrane represented the gut lumen and lamina propria, respectively, and assays were performed in the A-B and B-A directions (Figs. 3 and S10, respectively).

For all of the SLNs and emulsion, the P_{app} in the A-B direction (Fig. 3) was almost threefold larger than that in the B-A direction (Fig. S11), indicating passive transport of curcumin through the membrane (Hubatsch et al., 2007). In both the A-B and B-A directions (Figs. 3 and S10), P_{app} increased in the nontreated, bile-treated, and bile/lipase-treated samples, except the samples where curcumin was dissolved in 5 vol% ethanol. In the A-B direction, the P_{app} without was larger than that with a mucus layer (Fig. 3a and b). However, these values differed only slightly between the 17.1 and 46.9 mM PEG100SE-stabilized SLNs, indicating a negligible effect of the mucus layer. All of the chylomicrons secreted to the basolateral side of Caco-2 cells (Fig. S12) were submicron-sized and polyhedral. The chylomicrons of the 46.9 mM PEG100SE-stabilized SLNs were larger than the mixed micelles formed therefrom.

3.4. Pharmacokinetics of curcumin

The curcumin level in plasma isolated from the rat tail vein was recorded (Fig. 4). Most groups had low curcumin concentrations (< 58 ng mL $^{-1}$) for 9 h, with the exception of the two groups with PEG100SE-stabilized SLNs. The groups with 17.1 and 46.9 mM PEG100SE-stabilized SLNs had the largest C_{max} values (108 and 103 ng mL $^{-1}$, respectively), around sixfold that of curcumin in 5 vol% ethanol (EtOH), despite receiving half of the dose (25 mg kg $^{-1}$) of the EtOH group (50 mg kg $^{-1}$). The remaining groups had similarly low concentrations (≤ 29 ng mL $^{-1}$). Additionally, for most groups, t_{max} , the time to reach C_{max} , was 15 min, but it was 30 and 45 min for the groups administered 17.1 and 46.9 mM PEG100SE-stabilized SLNs, respectively. Based on the plasma level of curcumin, the pharmacokinetics,

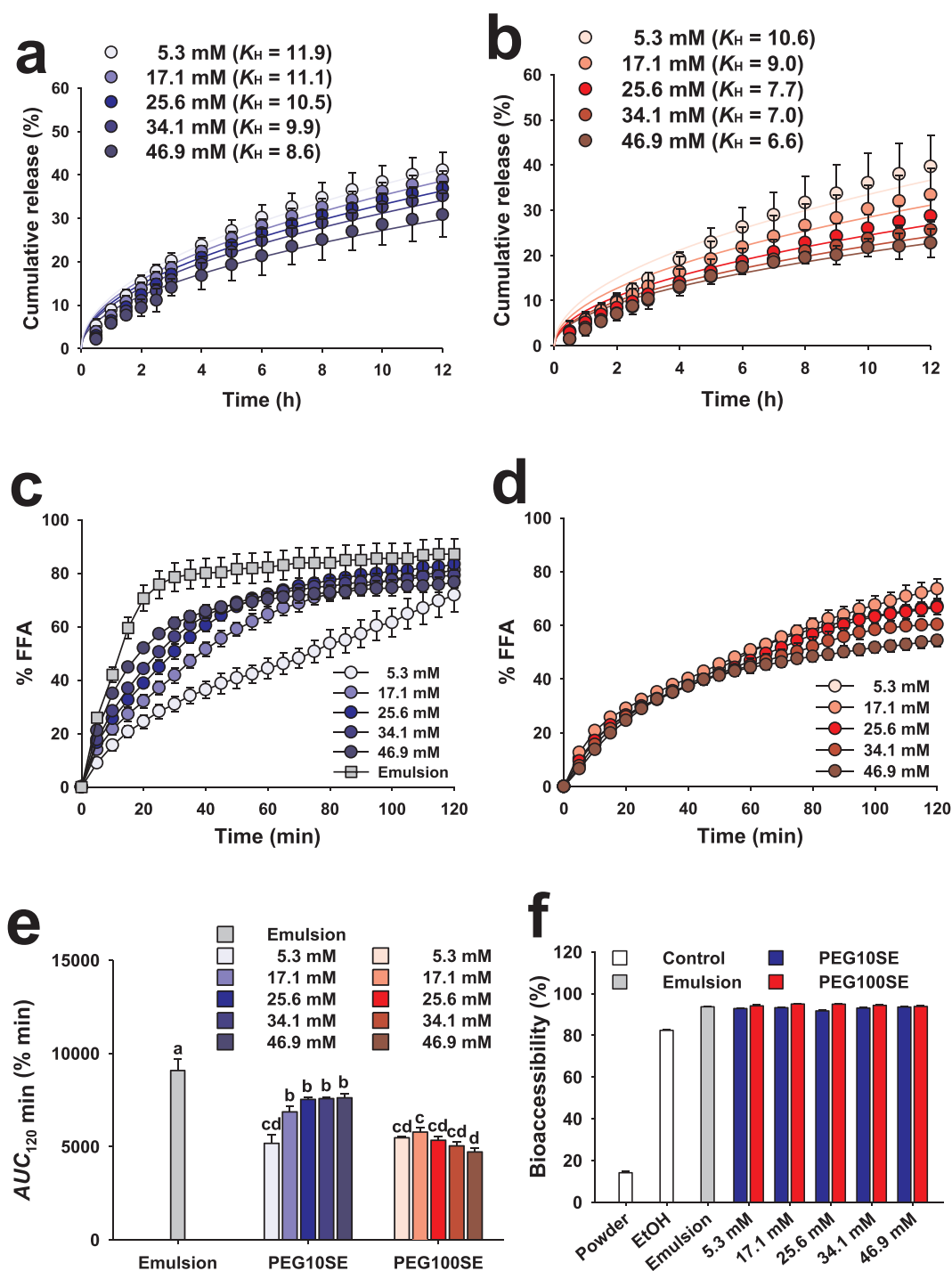


Fig. 2. Digestion of curcumin-loaded TS nanoparticles under simulated *in vitro* gastrointestinal tract (GIT) conditions. Cumulative profiles and fitting curves (Higuchi equation) of curcumin released from TS nanoparticles stabilized by (a) PEG10SE and (b) PEG100SE in the enzyme-free *in vitro* digestion medium using a dialysis membrane in sink conditions (50 vol% ethanol). Percentage of free fatty acids (%FFA) released from curcumin-loaded TS nanoparticles and emulsion stabilized by (c) PEG10SE and (d) PEG100SE in the simulated small intestine, according to the emulsifier concentration and (e) area under the curve for 120 min ($AUC_{120\text{ min}}$; different letters a-d indicate significant differences at $p < 0.05$ by Tukey's test). (f) Percentage of soluble curcumin in the digested micellar fraction after simulated *in vitro* digestion in the GIT (powder, powdered curcumin in phosphate-buffered saline; EtOH, curcumin dissolved in ethanol; emulsion, curcumin-loaded liquid canola oil (LCO) emulsion stabilized by 46.9 mM PEG10SE; PEG10SE and PEG100SE, curcumin-loaded TS nanoparticles stabilized by PEG10SE and PEG100SE, respectively).

including the $AUC_{0-9\text{h}}$ and $AUC_{0-\infty}$, were determined (Table 2). The groups with 17.1 and 46.9 mM PEG100SE-stabilized SLNs had significantly larger $AUC_{0-9\text{h}}$ and $AUC_{0-\infty}$ values ($AUC_{0-9\text{h}}$: 127 and 139 $\text{h}^*\text{ng mL}^{-1}$; $AUC_{0-\infty}$: 251 and 275 $\text{h}^*\text{ng mL}^{-1}$) than the other groups ($AUC_{0-9\text{h}}$: 28–78 $\text{h}^*\text{ng mL}^{-1}$; $AUC_{0-\infty}$: 34–82 $\text{h}^*\text{ng mL}^{-1}$). Compared to the EtOH group, the relative bioavailability of curcumin

based on the $AUC_{0-\infty}$ was greater in the groups with 17.1 and 46.9 mM PEG100SE-stabilized SLNs (12.0 and 13.2, respectively), but was smaller in the other groups (1.6–2.3).

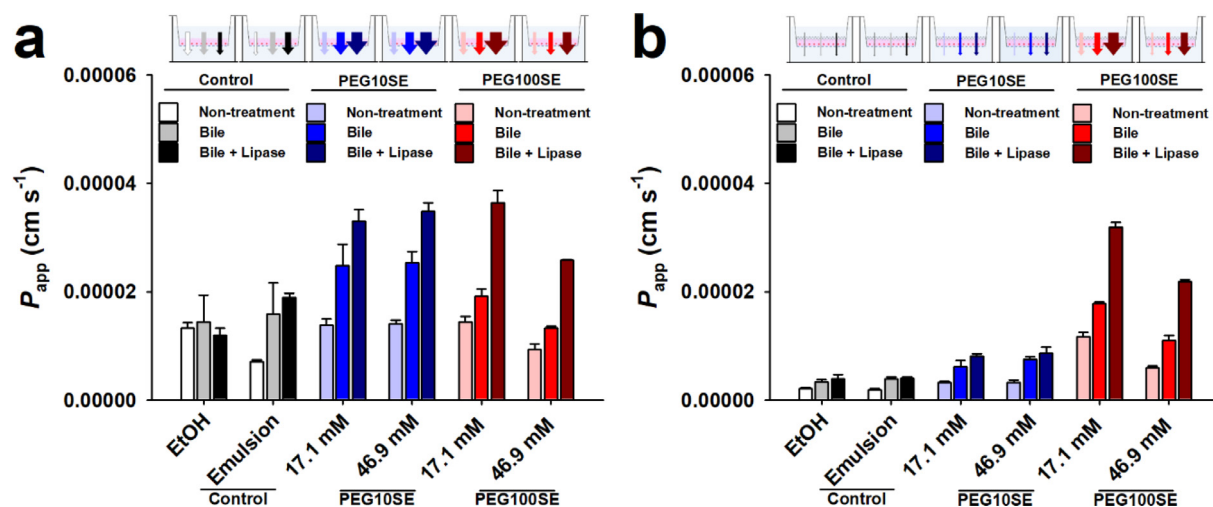


Fig. 3. Apparent permeation rates (P_{app}) of curcumin solubilized in ethanol (EtOH), incorporated into the LCO emulsion (stabilized by 46.9 mM PEG10SE) and loaded in the TS nanoparticles stabilized by PEG10SE and PEG100SE through the Caco-2 cell monolayer. Apical to basolateral side (a) without or (b) with an artificial mucus layer. Arrows, flux of curcumin.

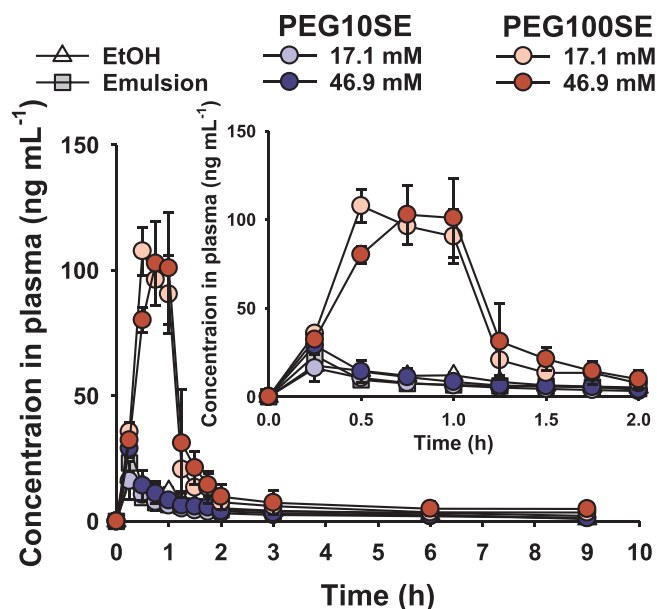


Fig. 4. Concentration of curcumin in plasma collected from the caudal vein of rats ($n = 9$) orally administered the curcumin formulations (EtOH, curcumin dissolved in EtOH; emulsion, curcumin-loaded LCO emulsion stabilized by 46.9 mM PEG10SE; PEG10SE and PEG100SE, curcumin-loaded TS nanoparticles stabilized by PEG10SE and PEG100SE).

Table 2

Pharmacokinetic parameters (C_{max} , t_{max} , AUC_{0-9h} , $AUC_{0-\infty}$, and relative bioavailability^a) of different curcumin formulations.

Samples	Surfactant concentration (mM)	Curcumin dose (mg kg ⁻¹)	C_{max} (ng mL ⁻¹)	t_{max} (h)	AUC_{0-9h} (h*ng mL ⁻¹)	$AUC_{0-\infty}$ (h*ng mL ⁻¹)	Relative bioavailability
EtOH ^b	–	50	18 ± 3c	0.25	40 ± 4bc	42 ± 4b	1.0
Emulsion ^c	46.9	25	23 ± 4c	0.25	40 ± 5bc	47 ± 6b	2.3
PEG10SE	17.1	25	16 ± 8c	0.25	28 ± 9c	34 ± 12b	1.6
	46.9	25	29 ± 3c	0.25	38 ± 6b	44 ± 9b	2.1
PEG100SE	17.1	25	108 ± 10a	0.50	127 ± 16a	251 ± 36a	12.0
	46.9	25	103 ± 17a	0.75	139 ± 42a	275 ± 81a	13.2

Different letters a–c in a column are significantly different at $p < 0.05$. C_{max} , peak concentration; t_{max} , time to reach the C_{max} ; AUC_{0-9h} , area under the plasma concentration-time curve from 0 to 9 h; and $AUC_{0-\infty}$, area under the curve from 0 h to ∞ .

^a The value of $AUC_{0-\infty}$ per dose when the value of $AUC_{0-\infty}$ per dose for the EtOH sample is fixed as 1.0.

^b Curcumin diluted in 5% (v/v) ethanol.

^c Curcumin-loaded emulsion prepared with liquid canola oil and 46.9 mM of PEG10SE.

4. Discussion

Colloids are easily influenced by the conditions of the dispersed phase, such as pH and ions. Specifically, changes in the pH/ionic conditions during gastrointestinal digestion can cause undesirable results, such as aggregation (McClements & Li, 2010), which might induce unpredictable digestion. In this study, the physicochemical characteristics of curcumin-loaded SLNs were similar to those of blank SLNs fabricated using the same materials and methods (Ban et al., 2018). The minor difference in reduction of ZP is likely attributable to the small amount of curcumin in the surficial area of the SLNs. Because of this, the colloidal stability of the > 5.3 mM emulsifier-stabilized SLNs was good under high ionic strength/acidic conditions, and following treatment with bile extract, pancreatic lipase, or both, as was the lipolysis pattern (Fig. 1). Oil droplets stabilized by nonionic surfactants were relatively stable under high-ionic-strength/acidic conditions (Mun, Decker, & McClements, 2007). Moreover, the nonionic surfactant-stabilized SLNs are not aggregated by positively charged divalent ions (Golding & Wooster, 2010). Therefore, the curcumin-loaded SLNs and emulsion can pass through the mouth and stomach and reach the small intestine without aggregation.

Bile acids play a role in eliminating steric hindrance by replacing surfactants on the surface (Maldonado-Valderrama, Wilde, Macierzanka, & Mackie, 2011), resulting in adsorption of the pancreatic lipase and colipase complex. In this regard, preventing the adsorption of BAs on the surface could be used to control lipolysis. In the small intestine, triacylglycerol is hydrolyzed to monoacylglycerol and two fatty acids by pancreatic lipase, aggregates with phospholipids and BAs,

forms mixed micelles, and is finally absorbed into the circulatory system via the mucus-covered epithelium (Shi & Burn, 2004). Therefore, the uptake of curcumin in SLNs into the circulatory system is dependent on micelle formation and absorption via the mucus-covered gut epithelium. Lipolysis governs micelle formation because lipolysate is the building block of micelles. Lipolysis in the small intestine was modulated by controlling the size and interfacial properties of the SLNs, such as the molecular weight of the emulsifiers and Γ_s (linked to the emulsifier concentration; Fig. 2c–e). Additionally, as the use of liquid oil (LCO in this case) increased the lipolysis rate, the lipid type also affected lipolysis. As verified by the bioaccessibility(%) (Fig. 2f), most of the curcumin loaded in the SLNs or emulsion was dissolved in the mixed micelles after digestion. In summary, during the controlled digestion of SLNs/emulsion in the small intestine, curcumin in mixed micelles was immediately accessible to pass through the gut epithelium.

Goblet cells secrete mucin into the gut lumen. The mucin forms a gel that covers the gut epithelial membrane as a mucus layer, and acts as a barrier to pathogens, toxins, and endogenous substances (Cone, 2009). The mucin gel comprises hydrophobic-nonglycosylated and hydrophilic-glycosylated domains and is negatively charged due to sialic acids. The mucus layer constitutes dynamic, steric, and interactive barriers to the gut epithelial permeation as a size exclusion filter or a hydrophobic, ionic, hydrophobic, and hydrogen-bonding gel-structure (Boegh & Nielsen, 2015). Therefore, the mucus layer plays a critical role in nutrient absorption through the epithelium. The mucus-covered gut epithelium has been simulated using various substances, such as *ex vivo* porcine intestine with a mucus layer (Bajka, Rigby, Cross, Macierzanka, & Mackie, 2015), a Caco-2 cell monolayer cocultured with mucus-secreting HT29 cells (Ensign, Schneider, Suk, Cone, & Hanes, 2012), and a Caco-2 cell monolayer covered with porcine intestinal mucus (Boegh et al., 2014). However, these simulations had various issues, associated with variation among individual porcine intestines, differences compared to human mucus, and the toxicity of the porcine mucus to the epithelium. The intestinal epithelium model used in this study effectively mimicked the mucus-covered intestinal barrier (Fig. S8).

In a previous study involving Caco-2 cell membranes, increases in the P_{app} of drugs were observed after BA treatment to drug-loaded lipid droplets, or after mixed micelle formation (Kotake-Nara & Nagao, 2012). A similar trend was observed in this study (Fig. 3). Penetration of lipid particles across the gut epithelium is dependent on their size and surface chemistry, due to the steric/interactive barrier of the mucus layer (Boegh & Nielsen, 2015). Specifically, the surface chemistry of the particles is a critical determinant of their diffusivity in the presence of a mucus layer on the epithelium (Lai, Wang, & Hanes, 2009). The diffusivity of COOH-coated particles (100, 200, and 500 nm) was decreased by a mucus layer covering the epithelium, but that of PEG-coated particles (200 and 500 nm) changed little. Particles coated with PEG of $< \sim 5.5$ kDa with a $ZP > \sim -8$ mV were defined as non-mucoadhesive. In this study (Fig. 1), the nontreated, bile-treated, and bile/lipase-treated SLNs stabilized by ≥ 17.1 mM PEG100SE and the nontreated emulsion can be defined as non-mucoadhesive and non-mucorepulsive, and the difference in P_{app} according to the absence or presence of a mucus layer was minimal, except in the nontreated emulsion (Fig. 3). The large difference in the nontreated emulsion might be due to the size being too small, at 112 nm (Lai et al., 2009).

After the uptake of the mixed micelles into enterocytes, fatty acids and monoacylglycerols are converted into triacylglycerols, transformed into chylomicrons with cholesterols and apoproteins, and transported to the lymphatic system through lacteals (Shi & Burn, 2004). In this study, chylomicron-like particles were observed in the basolateral compartment (Fig. S12). The chylomicron-like particles were slightly larger than the Caco-2 chylomicrons (80–200 nm) (Nauli et al., 2014), possibly due to stearic acid being digested from TS instead of oleic acid, linoleic acid, or linolenic acid (Yao, McClements, Zhao, Craig, & Xiao, 2017). Therefore, the curcumin in mixed micelles could be absorbed by enterocytes, incorporated into chylomicrons, and transported into the

circulatory system through lacteals (Fig. 4 and Table 2). The large bioavailability values (12.0 and 13.2) for 17.1 and 46.9 mM PEG100SE-stabilized SLNs could be attributed to their ability to pass through the mucus layer, in turn due to their neutral surface charge.

Fig. S13 summarizes the absorption mechanisms of curcumin loaded in SLNs and emulsion. Despite the high bioaccessibility(%), raw curcumin poorly permeated the mucus layer; most was excreted in feces, resulting in low bioavailability. Due to the poor permeability of the mixed micelles across the mucus-covered epithelium, curcumin loaded in the PEG10SE-stabilized SLNs/emulsion had relatively low bioavailability despite greater formation of mixed micelles. In contrast, the good permeability of the PEG100SE-stabilized SLNs across the mucus-covered epithelium explains their high bioavailability, despite the less marked mixed micelle formation. Consequently, the uptake rate and OBA of curcumin administered into the circulatory system could be controlled by changing the parameters of the encapsulation system, such as the type of lipid and emulsifiers, and the emulsifier concentration.

5. Conclusion

Solid lipid nanoparticles designed to control the absorption of orally administered curcumin were prepared with TS and a PEGylated emulsifier (PEG10SE or PEG100SE). Under GIT conditions, digestion of the curcumin-loaded SLNs was modulated by controlling the interfacial properties of the SLNs, such as the interface thickness, PS, and Γ_s . Most of the curcumin encapsulated in the SLNs was solubilized in mixed micelles after digestion. The size and surface charge of the mixed micelles influenced their permeability across the mucus-covered small-intestinal epithelium *in vitro*, which in turn affected the plasma curcumin level. Both the interfacial properties of the SLNs and the size/charge of the mixed micelles were determined by the molecular weight and concentration of the emulsifiers used, and the SLN formulation modulated the absorption of curcumin. Consequently, the OBA of curcumin encapsulated in PEG100SE-stabilized SLNs was improved due to prolonged lipolysis of the SLNs and the adequate size and neutral surface charge of the mixed micelles in the small intestine. This study may facilitate the development of an oral delivery system for poorly bioavailable molecules, with potential applications in functional foods and pharmaceuticals.

Declaration of Competing Interest

The authors declare that they have no known competing financial interests or personal relationships that could have appeared to influence the work reported in this paper.

Acknowledgements

This research was supported by Basic Science Research Program through the National Research Foundation of Korea (NRF) funded by the Ministry of Science, ICT and Future Planning (NRF-2018R1D1A1B07050508 and NRF-2017R1A6A1A03015642).

Appendix A. Supplementary data

Supplementary data to this article can be found online at <https://doi.org/10.1016/j.foodchem.2019.125328>.

References

- Anand, P., Kunnumakkara, A. B., Newman, R. A., & Aggarwal, B. B. (2007). Bioavailability of curcumin: Problems and promises. *Molecular Pharmaceutics*, 4(6), 807–818.
- Baek, J.-S., & Cho, C.-W. (2017). Surface modification of solid lipid nanoparticles for oral delivery of curcumin: Improvement of bioavailability through enhanced cellular uptake, and lymphatic uptake. *European Journal of Pharmaceutics and*

- Biopharmaceutics*, 117, 132–140.
- Bajka, B. H., Rigby, N. M., Cross, K. L., Macierzanka, A., & Mackie, A. R. (2015). The influence of small intestinal mucus structure on particle transport *ex vivo*. *Colloids and Surfaces B: Biointerfaces*, 135, 73–80.
- Ban, C., Jo, M., Lim, S., & Choi, Y. J. (2018). Control of the gastrointestinal digestion of solid lipid nanoparticles using PEGylated emulsifiers. *Food Chemistry*, 239, 442–452.
- Ban, C., Lim, S., Chang, P., & Choi, Y. J. (2014). Enhancing the stability of lipid nanoparticle systems by sonication during the cooling step and controlling the liquid oil content. *Journal of Agricultural and Food Chemistry*, 62(47), 11557–11567.
- Ban, C., Park, S. J., Lim, S., Choi, S. J., & Choi, Y. J. (2015). Improving flavonoid bioaccessibility using an edible oil-based lipid nanoparticle for oral delivery. *Journal of Agricultural and Food Chemistry*, 63(21), 5266–5272.
- Baspınar, Y., Üstündaş, M., Bayraktar, O., & Sezgin, C. (2018). Curcumin and piperine loaded zein-chitosan nanoparticles: Development and *in-vitro* characterisation. *Saudi Pharmaceutical Journal*, 26(3), 323–334.
- Boegh, M., Baldursdóttir, S. G., Müllertz, A., & Nielsen, H. M. (2014). Property profiling of biosimilar mucus in a novel mucus-containing *in vitro* model for assessment of intestinal drug absorption. *European Journal of Pharmaceutics and Biopharmaceutics*, 87, 227–235.
- Boegh, M., & Nielsen, H. M. (2015). Mucus as a barrier to drug delivery – understanding and mimicking the barrier properties. *Basic & Clinical Pharmacology & Toxicology*, 116, 179–186.
- Cone, R. A. (2009). Barrier properties of mucus. *Advanced Drug Delivery Reviews*, 61, 75–85.
- Devraj, R., Williams, H. D., Warren, D. B., Mullertz, A., Porter, C. J. H., & Pouton, C. W. (2013). *In vitro* digestion testing of lipid-based delivery systems: Calcium ions combine with fatty acids liberated from triglyceride rich lipid solutions to form soaps and reduce the solubilization capacity of colloidal digestion products. *International Journal of Pharmaceutics*, 441, 323–333.
- Ensign, L. M., Schneider, C., Suk, J. S., Cone, R., & Hanes, J. (2012). Mucus penetrating nanoparticles: Biophysical tool and method of drug and gene delivery. *Advanced Materials*, 24, 3887–3894.
- Golding, M., & Wooster, T. J. (2010). The influence of emulsion structure and stability on lipid digestion. *Current Opinion in Colloid & Interface Science*, 15, 90–101.
- Hartono, S. B., Hadioewignyo, L., Yang, Y., Meka, A. K., & Yu, C. (2016). Amine functionalized cubic mesoporous silica nanoparticles as an oral delivery system for curcumin bioavailability enhancement. *Nanotechnology*, 27(50), 505605.
- Higuchi, T. (1963). Mechanism of sustained-action medication. Theoretical analysis of rate of release of solid drugs dispersed in solid matrices. *Journal of Pharmaceutical Sciences*, 52(12), 1145–1149.
- Hubatsch, I., Ragnarsson, E. G. E., & Artursson, P. (2007). Determination of drug permeability and prediction of drug absorption in Caco-2 monolayers. *Nature Protocols*, 2(9), 2111–2119.
- Ji, H., Tang, J., Li, M., Ren, J., Zheng, N., & Wu, L. (2016). Curcumin-loaded solid lipid nanoparticles with Brij78 and TPGS improved *in vivo* oral bioavailability and *in situ* intestinal absorption of curcumin. *Drug Delivery*, 23(2), 459–470.
- Julie, S., & Jurenka, M. T. (2009). Anti-inflammatory properties of curcumin, a major constituent. *Alternative Medicine Review*, 14(2), 141–153.
- Kotake-Nara, E., & Nagao, A. (2012). Effects of mixed micellar lipids on carotenoid uptake by human intestinal Caco-2 cells. *Bioscience, Biotechnology, and Biochemistry*, 76(5), 875–882.
- Kunchandy, E., & Rao, M. N. A. (1990). Oxygen radical scavenging activity of curcumin. *International Journal Pharmaceutics*, 58(3), 237–240.
- Lai, S. K., Wang, Y.-Y., & Hanes, J. (2009). Mucus-penetrating nanoparticles for drug and gene delivery to mucosal tissues. *Advanced Drug Delivery Reviews*, 61, 158–171.
- Maldonado-Valderrama, J., Wilde, P., Macierzanka, A., & Mackie, A. (2011). The role of bile salts in digestion. *Advances in Colloid and Interface Science*, 165, 36–46.
- McClements, D. J., & Li, Y. (2010). Structured emulsion-based delivery systems: Controlling the digestion and release of lipophilic food components. *Advances in Colloid and Interface Science*, 159, 213–228.
- McClements, D. J., & Xiao, H. (2012). Potential biological fate of ingested nanoemulsions: Influence of particle characteristics. *Food & Function*, 3, 202–220.
- Metzler, M., Pfeiffer, E., Schulz, S. I., & Dempe, J. S. (2013). Curcumin uptake and metabolism. *Biofactors*, 39, 14–20.
- Mun, S., Decker, E. A., & McClements, D. J. (2007). Influence of emulsifier type on *in vitro* digestibility of lipid droplets by pancreatic lipase. *Food Research International*, 40, 770–781.
- Nauli, A. M., Sun, Y., Whittimore, J. D., Atyia, S., Krishnaswamy, G., & Nauli, S. M. (2014). Chylomicrons produced by Caco-2 cells contained ApoB-48 with diameter of 80–200 nm. *Physiological Reports*, 2(6), e12018.
- Ono, K., Hasegawa, K., Naiki, H., & Yamada, M. (2004). Curcumin has potent anti-amyloidogenic effects for Alzheimer's β -amyloid fibrils *in vitro*. *Journal of Neuroscience Research*, 75(6), 742–750.
- Peng, S., Zou, L., Liu, W., Li, Z., Liu, W., Hu, X., ... Liu, C. (2017). Hybrid liposomes composed of amphiphilic chitosan and phospholipid: Preparation, stability and bioavailability as a carrier for curcumin. *Carbohydrate Polymers*, 156, 322–332.
- Schneider, C., Gordon, O. N., Edwards, R. L., & Luis, P. B. (2015). Degradation of curcumin: From mechanism to biological implications. *Journal of Agricultural and Food Chemistry*, 63(35), 7606–7614.
- Sharma, R. A., Euden, S. A., Platton, S. L., Cooke, D. N., Shafayat, A., Hewitt, H. R., ... Plummer, S. M. (2004). Phase I clinical trial of oral curcumin biomarkers of systemic activity and compliance. *Clinical Cancer Research*, 10, 6847–6854.
- Shi, Y., & Burn, P. (2004). Lipid metabolic enzymes: Emerging drug targets for the treatment of obesity. *Nature Reviews Drug Discovery*, 3, 695–710.
- Shoba, G., Joy, D., Joseph, T., Majeed, M., Rajendran, R., & Srinivas, P. S. (1998). Influence of piperine on the pharmacokinetics of curcumin in animals and human volunteers. *Planta Medica*, 64(4), 353–356.
- Strimpakos, A. S., & Sharma, R. A. (2008). Curcumin: Preventive and therapeutic properties in laboratory studies and clinical trials. *Antioxidants & Redox Signaling*, 10(3), 511–546.
- Tadros, T., Izquierdo, P., Esquena, J., & Solans, C. (2004). Formation and stability of nano-emulsions. *Advances in Colloid and Interface Science*, 108–109, 303–318.
- Vecchione, R., Quagliarello, V., Calabria, D., Calcagno, V., De Luca, E., Iaffaioli, R. V., & Netti, P. A. (2016). Curcumin bioavailability from oil in water nano-emulsions: *In vitro* and *in vivo* study on the dimensional, compositional and interactional dependence. *Journal of Controlled Release*, 233, 88–100.
- Wahlang, B., Pawar, Y. B., & Bansal, A. K. (2011). Identification of permeability-related hurdles in oral delivery of curcumin using the Caco-2 cell model. *European Journal of Pharmaceutics and Biopharmaceutics*, 77, 275–282.
- Wang, Y. J., Pan, M. H., Cheng, A. L., Lin, L. I., Ho, Y. S., Hsieh, C. Y., & Lin, J. K. (1997). Stability of curcumin in buffer solutions and characterization of its degradation products. *Journal of Pharmaceutical and Biomedical Analysis*, 15, 1867–1876.
- Yao, M., McClements, D. J., Zhao, F., Craig, R. W., & Xiao, H. (2017). Controlling the gastrointestinal fate of nutraceutical and pharmaceutical-enriched lipid nanoparticles: From mixed micelles to chylomicrons. *NanoImpact*, 5, 13–21.
- Zhang, Z., Zhang, R., Zou, L., Chen, L., Ahmed, Y., Al Bishri, W., ... McClements, D. J. (2016). Encapsulation of curcumin in polysaccharide-based hydrogel beads: Impact of bead type on lipid digestion and curcumin bioaccessibility. *Food Hydrocolloids*, 58, 160–170.